JACS
JOURNAL OF THE AMERICAN CHEMICAL SOCIETY
Communication
pubs.acs.org/JACS

Synergetic Effect of MoS_2 and Graphene as Cocatalysts for Enhanced Photocatalytic H_2 Production Activity of TiO_2 Nanoparticles

Quanjun Xiang,[†] Jiaguo Yu,*[,†] and Mietek Jaroniec*[,‡]

[†]State Key Laboratory of Advanced Technology for Material Synthesis and Processing, Wuhan University of Technology, 122 Luoshi Road, Wuhan 430070, P. R. China

[‡]Department of Chemistry, Kent State University, Kent, Ohio 44242, United States

Supporting Information

ABSTRACT: The production of H_2 by photocatalytic water splitting has attracted a lot attention as a clean and renewable solar H_2 generation system. Despite tremendous efforts, the present great challenge in materials science is to develop highly active photocatalysts for splitting of water at low cost. Here we report a new composite material consisting of TiO_2 nanocrystals grown in the presence of a layered MoS_2/graphene hybrid as a high-performance photocatalyst for H_2 evolution. This composite material was prepared by a two-step simple hydrothermal process using sodium molybdate, thiourea, and graphene oxide as precursors of the MoS_2/graphene hybrid and tetrabutylorthotitanate as the titanium precursor. Even without a noble-metal cocatalyst, the TiO_2/MoS_2/graphene composite reaches a high H_2 production rate of 165.3 μmol h^{-1} when the content of the MoS_2/graphene cocatalyst is 0.5 wt % and the content of graphene in this cocatalyst is 5.0 wt %, and the apparent quantum efficiency reaches 9.7% at 365 nm. This unusual photocatalytic activity arises from the positive synergetic effect between the MoS_2 and graphene components in this hybrid cocatalyst, which serve as an electron collector and a source of active adsorption sites, respectively. This study presents an inexpensive photocatalyst for energy conversion to achieve highly efficient H_2 evolution without noble metals.

The production of chemical fuels by solar energy conversion has been considered as one of the major strategies for solving the global energy problem.[1,2] Since the pioneering report by Fujishima and Honda[3] on photoelectrochemical water splitting on a TiO_2 electrode, this photocatalytic process has attracted a lot of attention and appears to be a promising strategy for clean, low-cost, and environmentally friendly production of H_2 by utilizing solar energy.[4] Among various oxide semiconductor photocatalysts, titania has proven to be a suitable candidate for photocatalytic water splitting because of its biological and chemical inertness, cost effectiveness, environmental friendliness, availability, and long-term stability against photo- and chemical corrosion.[5] Typically, the photocatalytic H_2 production activity on TiO_2 is strongly dependent on the type and amount of cocatalyst because bare TiO_2 has poor photocatalytic activity.[6] It is well-known that the loading of Pt as a cocatalyst on TiO_2 significantly enhances the H_2 production efficiency for photocatalytic water splitting in the presence of sacrificial reagents.[5a] However, Pt is a rare and expensive noble metal. Therefore, alternative cocatalysts based on nonprecious metals and metal-free materials have been actively pursued.

Graphene, a single layer of graphite, has been reported to be an efficient cocatalyst for photocatalytic H_2 production because of its high specific surface area and superior electron mobility.[7] However, the H_2 production activity of graphene based-photocatalysts must be further enhanced from the viewpoint of practical applications and commercial benefits. Recently, molybdenum disulfide (MoS_2) with a layered structure has been extensively investigated as a promising electrocatalyst for H_2 evolution.[8,9] To date, its potential as a cocatalyst for photocatalytic H_2 production has received only sporadic attention even though it has demonstrated high activity in reactions involving H_2 under heterogeneous catalysis.[9,10] For instance, Jaramillo et al.[9a] reported electrochemical H_2 production with the help of MoS_2 nanocatalysts and identified their active sites for H_2 evolution. Zong et al.[10b] reported enhancement of the photocatalytic H_2 production activity of CdS by loading MoS_2 as cocatalyst. Unfortunately, cadmium is a widespread environmental pollutant that is toxic and harmful to human beings. Recently, a MoS_2−TiO_2 system has been reported to show high photocatalytic performance for pollutant degradation.[11] In particular, Kanda et al.[10c] reported that MoS_2 nanoparticles (NPs) photodeposited on TiO_2 exhibited high photocatalytic activity toward H_2 generation. According to our knowledge, no prior work regarding the application of a MoS_2−TiO_2 composite photocatalyst with layered MoS_2 as a cocatalyst for H_2 evolution has been reported to date.

Here we report for the first time the synthesis of TiO_2 NPs on a layered MoS_2/graphene (MG) hybrid for use in photocatalytic H_2 production. It is shown that the activity of the TiO_2 NPs is significantly enhanced by the presence of this layered MG cocatalyst. In this case, ethanol was used as a sacrificial agent, as it is a sustainable and renewable source and showed very good performance with this photocatalyst; however, other sacrificial agents (e.g., glycerol) can be used to make this strategy feasible.

The TiO_2/MG composite photocatalyst was synthesized by a two-step hydrothermal process. In the first step, the layered MG hybrid was prepared by the hydrothermal reaction of

Received: March 23, 2012
Published: March 29, 2012

Na_2MoO_4 and H_2CSNH_2 in an aqueous solution of graphene oxide (GO) at 210 °C for 24 h [see the Supporting Information (SI) for details]. During this process, GO was reduced to graphene simultaneously with the dispersion of graphene-like MoS_2 nanosheets on graphene sheets (Figure S1 in the SI). Subsequent hydrothermal treatment of $Ti(OC_4H_9)_4$ and MG hybrid in an ethanol/water solvent led to crystallization of TiO_2 and formation of the TiO_2/MG composite (denoted as T/95M5.0G, which contains 99.5% TiO_2 and 0.5% cocatalyst consisting of MoS_2 (95%) and graphene (5.0%); for details, see Table S1 in the SI). Figure 1a,b shows transmission electron microscopy (TEM) images of the resulting TiO_2/MG composite, in which the layered MG serves as a novel support (Figure S1) that is uniformly decorated with TiO_2 NPs (see the schematic illustration of the microstructure of T/95M5.0G in Figure S2). The high-resolution TEM images in Figure 1c,d show the structure of the TiO_2, with an average crystallite size of 7−10 nm and disordered mesoporosity between nanocrystals, which was additionally confirmed by pore analysis based on N_2 adsorption measurements (Figure S3). The lattice fringes of individual TiO_2 NPs with a *d* spacing of 0.35 nm can be assigned to the (101) lattice planes of anatase TiO_2.[12] Notably, Figure 1c,d shows that the MG composite has a layered structure with interlayer spacings of ca. 0.62 and 0.34 nm, which correspond to the (002) and (001) planes of hexagonal MoS_2[13] and graphene,[14] respectively. Thus, a close neighborhood of TiO_2, MoS_2, and graphene components achieved by the hydrothermal processing is believed to favor the vectorial transfer of photogenerated electrons from TiO_2 to MoS_2 and/or graphene sheets, thus enhancing the charge separation and photocatalytic efficiency.

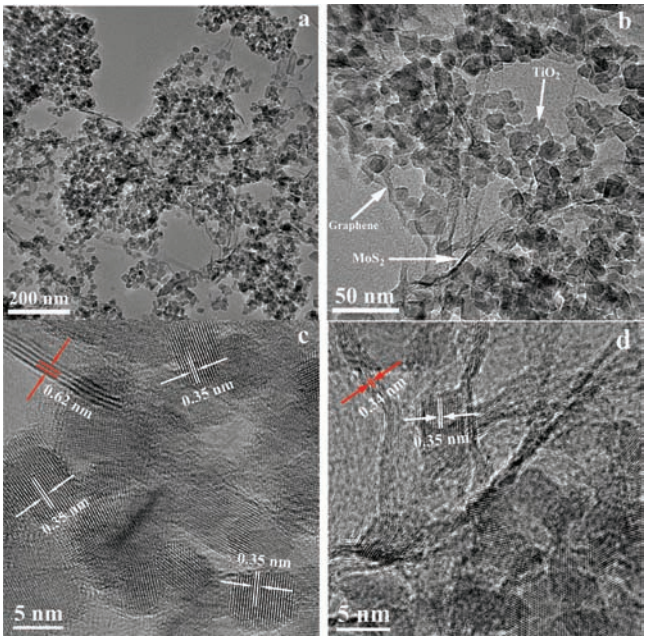

Figure 1. Structural analysis of the T/95M5.0G composite. (a, b) TEM images of TiO_2 NPs combined with layered MG hybrids. (c, d) High-resolution TEM images of TiO_2 nanocrystals grown on layered MG hybrids. The MG sheets can be considered as a support and interconnecting medium for the TiO_2 NPs.

The TiO_2/MG composite was characterized by powder X-ray diffraction (XRD); the diffraction peaks (Figure S4) match those of the crystalline anatase phase of TiO_2 (JCPDS no. 21-1272). X-ray photoelectron spectroscopy (XPS) revealed peaks for Ti, O, Mo, S, and C (Figure S5) with a Mo/S atomic ratio of ∼1:2, in good agreement with the nominal atomic composition of MoS_2. The high-resolution XPS spectrum (Figure S5 inset) shows the binding energies of the Mo $3d_{5/2}$ and Mo $3d_{3/2}$ peaks at 228.8 and 231.8 eV, respectively, which are typical values for Mo^{4+} in MoS_2.[15] In addition, the high-resolution XPS spectrum of C 1s proves the reduction of GO to graphene (Figure S6). To clarify this issue further, Raman analysis was performed. The Raman spectrum for the TiO_2/MoS_2/graphene composite (Figure 2) shows several characteristic bands at 148, 399, 518, and 639 cm^{-1}, corresponding to the $E_{g(1)}$, $B_{1g(1)}$, A_{1g} + $B_{1g(2)}$, and $E_{g(2)}$ modes of anatase,[16] respectively. Significantly, two bands at about 1343 cm^{-1} (D band) and 1586 cm^{-1} (G band) for the graphitized structures were also observed, confirming the presence of graphene in the TiO_2/MG composite. Also, the observed D and G bands of the composite are slightly shifted in comparison with the D band (1356 cm^{-1}) and G band (1596 cm^{-1}) of GO, and the D/G intensity ratio is larger, indicating the reduction of GO.[7c,17]

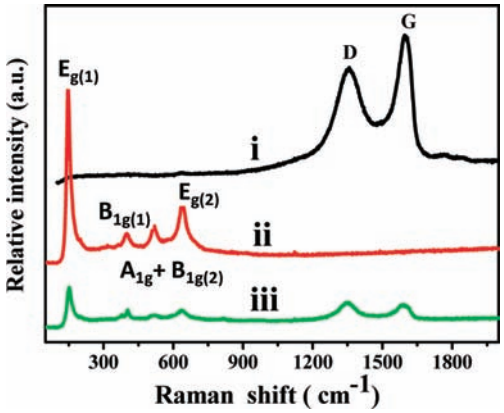

Figure 2. Raman spectra of (i) GO, (ii) anatase TiO_2, and (iii) the T/95M5.0G composite. In contrast to GO and TiO_2, the composite contained anatase TiO_2 and reduced GO.

The photocatalytic H_2 production activity on TiO_2 alone and on TiO_2/MG composite photocatalysts with different MoS_2 and graphene contents in the MG cocatalyst (denoted as T/100M0G, T/99M1.0G, T/95M5.0G, T/90M10G, and T/0M100G; for details, see Table S1) was evaluated under xenon arc lamp irradiation using ethanol as a scavenger (Figure 3). TiO_2 alone showed a very low photocatalytic activity because of the rapid recombination of conduction band (CB) electrons and valence band (VB) holes. The introduction of the layered MG cocatalyst resulted in a significant improvement in the photocatalytic H_2 production activity of TiO_2, and the content of graphene and MoS_2 in this cocatalyst had a significant influence on the photocatalytic activity. At zero graphene content, the composite photocatalyst with MoS_2 cocatalyst (T/100M0G) showed decent photocatalytic activity with a H_2 production rate of 36.8 μmol h^{-1}, because nanoscale MoS_2 can help in the charge separation and act as a cocatalyst for water reduction, thereby enhancing the photocatalytic H_2 production activity. In the presence of a small amount of graphene (1.0%) in the hybrid cocatalyst, the activity of the sample (T/99M1.0G) was enhanced to 76.7 μmol h^{-1}. When the graphene content reached 5.0% (T/95M5.0G), the H_2 production rate achieved the highest value of 165.3 μmol h^{-1}

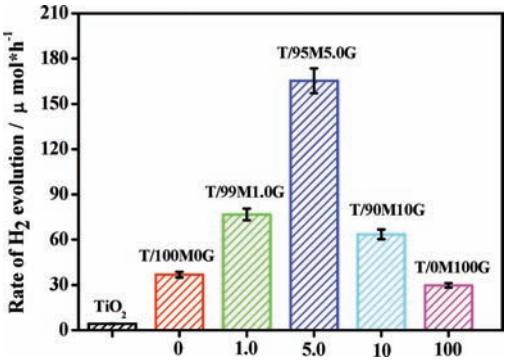

Figure 3. Photocatalytic H_2 evolution of TiO_2/MG composites. Photocatalytic H_2 production experiments were performed in 25% (v/v) ethanol/water solutions under UV irradiation using the photocatalyst TiO_2/MG composites with different MoS_2 and graphene contents in the MG hybrid as cocatalyst. The T/95M5.0G composite photocatalyst containing 95% MoS_2 and 5% graphene in the cocatalyst showed the highest H_2 production rate.

[corresponding to an apparent quantum efficiency (QE) of 9.7% at 365 nm], and the rate exceeded that obtained on TiO_2 alone and TiO_2 with MoS_2 cocatalyst (T/100M0G) by more than 39 and 4 times, respectively. Further increases in the graphene content in the cocatalyst led to a gradual reduction of the photocatalytic activity.

In the case of the T/0M100G composite photocatalyst having only graphene as the cocatalyst, the H_2 production rate decreased to 29.7 μmol h^{-1}. It should be noted that the latter value is still 7 times that obtained for TiO_2 alone, as graphene is an efficient cocatalyst for photocatalytic H_2 production because of its redox potential, which is less negative than the CB of TiO_2 and more negative than the H^+/H_2 potential (Figure S7), favoring electron transfer from the CB of TiO_2 to graphene and the reduction of H^+. Furthermore, the stability of T/95M5.0G was tested by using the same catalyst for photocatalytic H_2 production repeatedly four times (Figure S8). After four recycles, the catalyst did not exhibit any significant loss of activity, indicating its high stability during photocatalytic H_2 production.

A tentative mechanism proposed for the high H_2 production activity of the T/95M5.0G sample (95% MoS_2 and 5.0% graphene in the MG cocatalyst) is illustrated in Figure 4. Under UV illumination, the VB electrons of TiO_2 are excited to the CB, creating holes in the VB. Previous studies have shown that the CB electrons of TiO_2 can be injected into the graphene sheets in a graphene−TiO_2 system because the graphene/graphene$^{\bullet-}$ redox potential is slightly lower than the CB of anatase TiO_2 (Figure S7). The mobility of these electrons on the graphene sheets is high. The MoS_2 nanosheets in the MG hybrids can accept electrons and act as active sites for H_2 evolution.[2,8a,9a] In fact, nanoscale MoS_2 is highly active for H_2 evolution as a result of the quantum-confinement effect (Figure S7).[15b,c,18] The edges of the nanosized MoS_2 crystallites can promote the dissociation of water and the production of H_2.[8a,9a,10b] In summary, the photogenerated electrons in the CB of TiO_2 can be transferred to MoS_2 nanosheets through the graphene sheets (which act as a conductive electron transport "highway") and then react with the adsorbed H^+ ions at the edges of MoS_2 to form H_2. This indicates that because of a notable synergetic effect between MoS_2 nanosheets and graphene, the composite cocatalyst has several advantages, including suppression of charge recombination, improvement

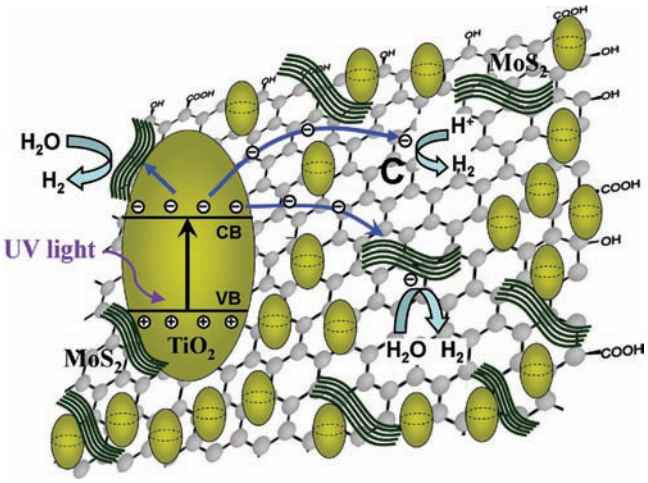

Figure 4. Schematic illustration of the charge transfer in TiO_2/MG composites. The proposed mechanism for the enhanced electron transfer in the TiO_2/MG system under irradiation assumes that the photoexcited electrons are transferred from the CB of TiO_2 not only to the MoS_2 nanosheets but also to the C atoms in the graphene sheets, which can effectively reduce H^+ to produce H_2.

of interfacial charge transfer, and an increase in the number of active adsorption sites and photocatalytic reaction centers. In addition, some photogenerated electrons can also be transferred directly to the MoS_2 nanosheets on the surface of TiO_2 or to C atoms on the graphene sheets, after which reaction with H^+ to produce H_2 is possible. Therefore, it is not surprising that TiO_2 with MoS_2 alone or graphene alone as cocatalyst shows decent photocatalytic H_2 production activity. Notably, the aforementioned three ways in which photogenerated electrons in the CB of TiO_2 are transferred improve the separation of the photogenerated electron−hole pairs, effectively prolong the lifetime of the charge carriers, enlarge the reaction space, and consequently enhance the photocatalytic activity for H_2 evolution. Transient photocurrent experiments (Figure S9) further demonstrated a noticeable improvement in the charge transport from TiO_2 to graphene and/or MoS_2 and then to the surface of the working electrode, additionally confirming the correctness of the suggested mechanism.

The experimental results discussed in this work highlight the synergetic effect of MoS_2 and graphene as cocatalysts that improve the photocatalytic H_2 production activity of TiO_2 NPs. Additionally, this study demonstrates that the layered composite material can be used as an effective cocatalyst for photocatalytic water splitting, which is a valuable indication for further development of related composite materials as substitutes for Pt in photocatalytic H_2 production.

To investigate the effect of the amount of the MG hybrid cocatalyst (95% MoS_2 and 5.0% graphene) on the photocatalytic H_2 production activity, a series of the TiO_2/MG composites with different amounts of hybrid cocatalyst [denoted as 99.8T/0.2(MG), 99.5T/0.5(MG), 99.0T/1.0(MG), and 97.0T/3.0(MG); for details, see Table S2] was examined in comparison to pure TiO_2 [denoted as 100T/0(MG)] and a mechanical mixture of 0.5% composite cocatalyst and 99.5% TiO_2 [denoted as 99.5T + 0.5(MG)]. The amount of cocatalyst has a significant influence on the photocatalytic activity of TiO_2 (Figure S10). Even with a small amount of cocatalyst (0.2−1.0 wt %), the H_2 production rate noticeably increased. The photocatalytic activity of the

composite increased with increasing amount of cocatalyst from 0.2 to 0.5% and reached a maximum H_2 production rate for the composite containing 0.5% hybrid cocatalyst. A further increase in the amount of cocatalyst led to a reduction of the activity. This is reasonable because the introduction of a slightly higher percentage of the black MG hybrid can lead to a significant increase in the opacity (see the color change in the Figure S11 inset), which reduces the UV absorption of TiO_2 (Figure S11).[7c,19] For comparison, the simple mechanical mixture of 0.5% MG hybrid and 99.5% TiO_2 showed a slightly higher H_2 production rate than TiO_2 alone. However, this mixture exhibited lower activity than the TiO_2/MG composite containing 0.5% MG cocatalyst, even though the amount of the latter in TiO_2 was the same. This fact indicates that simple mechanical mixing is not able to create effective interfacial contacts between the TiO_2, MoS_2, and graphene components (Figure S12), which seems to be crucial for the electron transfer between them.[4c,10b] In addition, control experiments detected no appreciable H_2 production when the MG hybrid alone was used as the catalyst (data not shown), suggesting that this hybrid is not active for photocatalytic H_2 production under the experimental conditions studied.

In summary, the proposed two-step hydrothermal synthesis of titania-based composite photocatalysts containing a layered MoS_2/graphene cocatalyst afforded an effective photocatalyst for H_2 production. The TiO_2/MG composite photocatalysts showed high photocatalytic H_2 production activity with a rate as high as 165.3 μmol h^{-1} for the sample containing 0.5% MG hybrid cocatalyst consisting of 95% MoS_2 and 5% graphene. The corresponding apparent QE reached 9.7% at 365 nm even without a noble-metal cocatalyst. It is believed that the positive synergetic effect between the MoS_2 and graphene sheets as the components of cocatalyst on the photocatalytic H_2 production activity can efficiently suppress charge recombination, improve interfacial charge transfer, and provide a greater number of active adsorption sites and photocatalytic reaction centers. This study shows that the development of noble-metal-free titania-based composites such as the present ones containing an inexpensive and environmentally benign MG hybrid cocatalyst is feasible and has a great potential for photocatalytic H_2 production.

■ ASSOCIATED CONTENT

Ⓢ Supporting Information

Experimental procedures and additional data. This material is available free of charge via the Internet at http://pubs.acs.org.

■ AUTHOR INFORMATION

Corresponding Author

jiaguoyu@yahoo.com; jaroniec@kent.edu

Notes

The authors declare no competing financial interest.

■ ACKNOWLEDGMENTS

This work was supported by the 973 Program (2009CB939704), NSFC (20877061 and 51072154), NSFHP (2010CDA078), and Innovative Research Funds of SKLWUT.

■ REFERENCES

(1) Paracchino, A.; Laporte, V.; Sivula, K.; Grätzel, M.; Thimsen, E. *Nat. Mater.* **2011**, *10*, 456.

(2) Hou, Y. D.; Abrams, B. L.; Vesborg, P. C. K.; Björketun, M. E.; Herbst, K.; Bech, L.; Setti, A. M.; Damsgaard, C. D.; Pedersen, T.; Hansen, O.; Rossmeisl, J.; Dahl, S.; Nørskov, J. K.; Chorkendorff, I. *Nat. Mater.* **2011**, *10*, 434.

(3) Fujishima, A.; Honda, K. *Nature* **1972**, *238*, 37.

(4) (a) Kudo, A.; Miseki, Y. *Chem. Soc. Rev.* **2009**, *38*, 253. (b) Maeda, K.; Xiong, A. K.; Yoshinaga, T.; Ikeda, T.; Sakamoto, N.; Hisatomi, T.; Takashima, M.; Lu, D. L.; Kanehara, M.; Setoyama, T.; Teranishi, T.; Domen, K. *Angew. Chem., Int. Ed.* **2010**, *49*, 4096. (c) Zhang, J.; Yu, J. G.; Zhang, Y. M.; Li, Q.; Gong, J. R. *Nano Lett.* **2011**, *11*, 4774.

(5) (a) Carp, O.; Huisman, C. L.; Reller, A. *Prog. Solid State Chem.* **2004**, *32*, 33. (b) Park, J. H.; Kim, S.; Bard, A. J. *Nano Lett.* **2006**, *6*, 24. (c) Ksibi, M.; Rossignol, S.; Tatibouet, J. M.; Trapalis, C. *Mater. Lett.* **2008**, *62*, 4204. (d) Yu, J. G.; Qi, L. F.; Jaroniec, M. *J. Phys. Chem. C* **2010**, *114*, 13118. (e) Liu, S. W.; Yu, J. G.; Jaroniec, M. *Chem. Mater.* **2011**, *23*, 4085.

(6) (a) Murdoch, M.; Waterhouse, G. I. N.; Nadeem, M. A.; Metson, J. B.; Keane, M. A.; Howe, R. F.; Llorca, J.; Idriss, H. *Nat. Chem.* **2011**, *3*, 489. (b) Yu, J. G.; Ran, J. R. *Energy Environ. Sci.* **2011**, *4*, 1364.

(7) (a) Lightcap, I. V.; Kosel, T. H.; Kamat, P. V. *Nano Lett.* **2010**, *10*, 577. (b) Li, Q.; Guo, B. D.; Yu, J. G.; Ran, J. R.; Zhang, B. H.; Yan, H. J.; Gong, J. R. *J. Am. Chem. Soc.* **2011**, *133*, 10878. (c) Xiang, Q. J.; Yu, J. G.; Jaroniec, M. *Nanoscale* **2011**, *3*, 3670. (d) Xiang, Q. J.; Yu, J. G. *Chem. Soc. Rev.* **2012**, *41*, 782. (e) Liang, Y. Y.; Li, Y. G.; Wang, H. L.; Zhou, J. G.; Wang, J.; Regier, T.; Dai, H. J. *Nat. Mater.* **2011**, *10*, 780.

(8) (a) Li, Y. G.; Wang, H. L.; Xie, L. M.; Liang, Y. Y.; Hong, G. S.; Dai, H. J. *J. Am. Chem. Soc.* **2011**, *133*, 7296. (b) Hinnemann, B.; Moses, P. G.; Bonde, J.; Jørgensen, K. P.; Nielsen, J. H.; Horch, S.; Chorkendorff, I.; Nørskov, J. K. *J. Am. Chem. Soc.* **2005**, *127*, 5308.

(9) (a) Jaramillo, T. F.; Jørgensen, K. P.; Bonde, J.; Nielsen, J. H.; Horch, S.; Chorkendorff, I. *Science* **2007**, *317*, 100. (b) Karunadasa, H. I.; Montalvo, E.; Sun, Y.; Majda, M.; Long, J. R.; Chang, C. J. *Science* **2012**, *335*, 698. (c) Bonde, J.; Moses, P. G.; Jaramillo, T. F.; Nørskov, J. K.; Chorkendorff, I. *Faraday Discuss.* **2008**, *140*, 219.

(10) (a) Moses, P. G.; Hinnemann, B.; Topsoe, H.; Nørskov, J. K. *J. Catal.* **2007**, *248*, 188. (b) Zong, X.; Yan, H. J.; Wu, G. P.; Ma, G. J.; Wen, F. Y.; Wang, L.; Li, C. *J. Am. Chem. Soc.* **2008**, *130*, 7176. (c) Kanda, S.; Akita, T.; Fujishima, M.; Tada, H. *J. Colloid Interface Sci.* **2011**, *354*, 607. (d) Frame, F. A.; Osterloh, F. E. *J. Phys. Chem. C* **2010**, *114*, 10628.

(11) (a) Araki, Y.; Honna, K.; Shimada, H. *J. Catal.* **2002**, *207*, 361. (b) Pourabbas, B.; Jamshidi, B. *Chem. Eng. J.* **2008**, *138*, 55. (c) Hu, K. H.; Hu, X. G.; Xu, Y. F.; Sun, J. D. *J. Mater. Sci.* **2010**, *45*, 2640. (d) Tacchini, I.; Terrado, E.; Ansón, A.; Martínez, M. T. *Micro Nano Lett.* **2011**, *6*, 932.

(12) Liu, S. W.; Yu, J. G.; Jaroniec, M. *J. Am. Chem. Soc.* **2010**, *132*, 11914.

(13) (a) Chang, K.; Chen, W. X.; Ma, L.; Li, H.; Li, H.; Huang, F. H.; Xu, Z. D.; Zhang, Q. B.; Lee, J. Y. *J. Mater. Chem.* **2011**, *21*, 6251. (b) Chang, K.; Chen, W. X. *J. Mater. Chem.* **2011**, *21*, 17175.

(14) Yeh, T. F.; Syu, J. M.; Cheng, C.; Chang, T. H.; Teng, H. S. *Adv. Funct. Mater.* **2010**, *20*, 2255.

(15) (a) Vanchura, B. A.; He, P. G.; Antochshuk, V.; Jaroniec, M.; Ferryman, A.; Barbash, D.; Fulghum, J. E.; Huang, S. D. *J. Am. Chem. Soc.* **2002**, *124*, 12090. (b) Ho, W. K.; Yu, J. C.; Lin, J.; Yu, J. G.; Li, P. S. *Langmuir* **2004**, *20*, 5865. (c) Yu, J.; Zhang, J.; Jaroniec, M. *Green Chem.* **2010**, *12*, 1611.

(16) (a) Yu, J. G.; Ma, T. T.; Liu, G.; Cheng, B. *Dalton Trans.* **2011**, *40*, 6635. (b) Yu, J. G.; Ma, T. T.; Liu, S. W. *Phys. Chem. Chem. Phys.* **2011**, *13*, 3491.

(17) Zhang, X. Y.; Li, H. P.; Cui, X. L.; Lin, Y. H. *J. Mater. Chem.* **2010**, *20*, 2801.

(18) (a) Thurston, T. R.; Wilcoxon, J. P. *J. Phys. Chem. B* **1999**, *103*, 11. (b) Linic, S.; Christopher, P.; Ingram, D. B. *Nat. Mater.* **2011**, *10*, 911.

(19) Xiang, Q. J.; Yu, J. G.; Jaroniec, M. *J. Phys. Chem. C* **2011**, *115*, 7355.